

Assessing the Potential for Pyroconvection and Wildfire Blow Ups

RYAN N. LEACH and CHRIS V. GIBSON
NOAA/National Weather Service, Missoula, Montana

(Manuscript received 28 October 2020; review completed 22 April 2021)

ABSTRACT

Fire meteorologists have few tools for assessing atmospheric stability in the context of wildfires. Most tools at our disposal were developed for assessing thunderstorms and general convection, and so they ignore heat and moisture supplied by the wildfire. We propose a simple parcel-based model that can be used to assess how the atmosphere will affect a growing wildfire plume by also taking into account the heat and moisture released from the fire. From this model, we can infer trends in day to day atmospheric stability as it relates to fire plumes. We can also infer how significant the appearance of a pyrocumulus cloud on the top of a fire column is. In some cases, the appearance of a pyrocumulus indicates that the fire is near if not already blowing up, whereas in other cases environmental conditions remain too stable to have a significant effect. A qualitative application of the model is demonstrated through application to a 2017 wildfire case in Western Montana.

1. Introduction

The Glossary of Meteorology defines a pyrocumulus cloud (pyroCu) as a cumulus cloud formed by a rising thermal from a fire, or enhanced by buoyant plume emissions from an industrial combustion process. A pyrocumulonimbus (pyroCb) cloud is defined as an extreme manifestation of a pyroCu cloud that often rises to the upper troposphere or lower stratosphere (American Meteorological Society 2021). A pyroCb can generate rain or lightning and may be glaciated. The World Meteorological Organization as early as 2017 defined these types of clouds as flammagenitus clouds (WMO 2017), though the more established pyroCu and pyroCb definitions from the American Meteorological Society are used in this paper. Although pyroCb is generally recognized as the most dangerous form of pyroconvection (Goens and Andrews 1998), the thermodynamics associated with the full range of pyroconvection are investigated in this paper. Henceforth, pyroCu will be used in this paper to refer to any cloud that is the result of pyroconvection because it is the more general term.

PyroCu and pyroCb clouds have been extensively studied since at least as early as the 1960's (Ebert

1963). Often, this research has been driven by interest in injection of aerosols and biomass into the lower stratosphere due to the potential implications on global climate (Luderer et al. 2006; Trentmann et al. 2006; Fromm et al. 2010; Peterson et al. 2015; Peterson et al. 2017). Less work has been done on the safety implications of pyroconvection and pyroCu clouds for firefighter safety and the occurrence of erratic fire behavior. Goens and Andrews (1998) described one of the most direct connections documented between cumulus convection and tragic consequences for firefighters. In addition, pyroCu may be related to extreme fire behavior in various ways by altering wind patterns near fires, generating dangerous lightning, and ultimately becoming severe thunderstorms (Cunningham and Reeder 2009), some of which may include tornadoes (Lareau et al. 2018). This paper proposes some relatively simple forecasting tools based on parcel analysis for forecasting the degree to which the atmosphere will support or inhibit pyroconvection.

The focus of this paper is on the thermodynamic role of the atmosphere in pyroconvection and the vertical extent of wildfire plumes. To analyze that, a simple parcel-based model is used. A fire plume can be thought of as being represented by a series of parcels

released near the surface with sensible and latent heat added from the fire. The resultant parcel will have the same properties as an environmental mixed layer parcel with the temperature warmed by ΔT as a result of the added sensible heat and an increased dewpoint due to the added latent heat. A mixed layer parcel is used initially due to the intense mixing occurring near the surface caused by the heat from the fire, which is similar to the approach taken by Tory et al. (2018) wherein they assumed a surface layer with constant specific humidity and potential temperature. Much can be gleaned by examining the thermodynamic properties of parcels with many different ΔT values.

Various parcel-based models have been used by many others who were investigating fire plumes including Potter (2002), Luderer et al. (2009), Fromm et al. (2010), Potter and Anaya (2015), Lareau and Clements (2016), Peterson et al. (2017), and Tory et al. (2018), among others. Uses have ranged from simple comparisons to the typical convective available potential energy (CAPE) used in meteorology (Fromm et al. 2010; Potter and Anaya 2015) to a detailed parcel-based model by Tory et al. (2018) that includes contributions from the fire, the near surface atmosphere, and entrainment of ambient air into the plume as it rises. Some notable results include Fromm et al. (2010), which observes that in some cases with pyroCu and pyroCb clouds there is 0 J/kg CAPE analyzed; and Lareau and Clements (2016), which observes that the analyzed convective condensation level (CCL) matches the cloud base of a pyroCb observed with LIDAR.

Moisture released by combustion of the surface fuels is a difficult challenge for this type of analysis, and it has been investigated by many others. Potter's (2005) thought experiment, the numerical simulations of Cunningham and Reeder (2009), and the model of Tory et al. (2018) all indicate that moisture contributed by the fire is important in the formation of pyroCu and pyroCb clouds. However, the numerical simulations of Trentmann et al. (2006), accompanied by the sensitivity study by Luderer et al. (2006), and followed by a more detailed theoretical analysis by Luderer et al. (2009), provide convincing evidence that moisture released by combustion can be safely ignored with relatively little practical impact to the results. Potter (2012b) reviews some earlier field studies which do measure increased moisture in fire plumes; however, these cases are not for the intense pyroconvection that poses a risk to firefighters and the public, for whom this study is concerned. Tory et al. (2018) took the approach to

assume a ratio of 1 g/kg moisture release from the fire into the plume for every 10K of heating based on the results of Luderer et al. (2009), and a similar approach is taken here by investigating the effects of releasing a range of moisture values.

Research thus far has not produced scientifically validated tools that weather forecasters can use to assess atmospheric stability as it relates to wildfire plumes and specifically pyroCu. Tory et al. (2018) developed an approach for assessing the conditions for pyroCu and pyroCb initiation, but they did not address a more general assessment of stability because they did not address the potential blow up of the plume. Numerical modeling and a simple parcel-based model are used below to explore fire-heated parcels with the ultimate goal of developing tools that forecasters can use to assess trends in atmospheric stability as they relate to wildfire plumes. These tools are then evaluated with a case study from a fire in western Montana.

2. Model development

We propose to use a simple parcel-based model where a surface-based 100 hPa thick mixed-layer parcel is heated by the fire, effectively increasing the temperature of the parcel. A mixed-layer parcel is used initially due to the intense mixing occurring near the surface caused by the heat from the fire, as discussed in section 1. The mixed-layer depth was chosen to be consistent with a common forecasting practice in meteorology, but more investigation may be necessary to find an optimal depth.

Moisture contributed by the fire is more difficult to specify, so Eq. (4) from Luderer et al. (2009) is utilized assuming 50% loss of heat generated by the fire through radiation and 10-60% average fuel moisture. The 50% radiative heat loss assumption may be high, but it is consistent with the numerical simulations by Luderer et al. (2009). Because of uncertainty related to moisture released by the fire, this study considers two scenarios where (1) no moisture is added to the fire, and (2) 1 g/kg specific humidity per 8 to 15°C of heating is added to each parcel, as in Luderer et al. (2009). These two unique moisture scenarios consider a reasonable range of uncertainty as supported by the literature outlined in section 1. See Luderer et al. (2009) for a more detailed explanation of this process as this is the most complete study we have found to date. All parcels are lifted dry adiabatically until they reach the condensation level,

and thereafter moist adiabatically just as it would be for any other parcel analysis.

Figure 1 shows an example of lifting four different parcels using a skew-T log-P diagram. As a parcel is lifted, the integrated buoyancy as a function of height as defined in Eq. (1) is tracked. In a typical parcel analysis for thunderstorms, the integrated buoyancy from the level of free convection to the Equilibrium Level (EL) is defined as the Convective Available Potential Energy (CAPE) as in Doswell (2001). It is important to differentiate this analysis from a typical stability analysis for thunderstorms; the integrated buoyancy from the surface to every level in the sounding is tracked in this case. Then, the Maximum Integrated Buoyancy (MIB) and the level of the MIB for a parcel as well as the Potential Maximum Plume Height (PMPH) are calculated from these values. The PMPH is defined as the level where the parcel has risen above the EL and integrated buoyancy reaches 0 J/kg again. The lifting condensation level (LCL) and EL are defined as usual and outlined in Fig. 1.1 of Doswell (2001). The level of the MIB is the same as the EL, however, there are cases where the plume must rise through a stable layer, as in parcels b and c in Fig. 1, and so there may be two ELs. Lifting a parcel through a stable layer causes the integrated buoyancy to decrease for a while before becoming positively buoyant upon reaching a layer where it is warmer than the environment again. In these cases when the parcel will go through two ELs, the EL with the highest integrated buoyancy and thus the level with the potentially strongest updraft is used.

Within this model, a blow up is defined as a sudden or discontinuous jump in the EL. Figure 2 shows the EL as a function of parcel heating for a typical example. Figure 2 does not account for latent heat added by the fire to keep the explanation simple; however, the results of doing so are shown later. The Blow Up (BU) ΔT is the amount of sensible heating needed from the fire to cause the EL to jump. The amount of the BU Δz is defined by the difference in the EL from the BU $\Delta T + 0.5^\circ\text{C}$ to BU $\Delta T - 0.5^\circ\text{C}$. In practice, the BU ΔT value is found by searching for the maximum value of the numerical derivative, but a fixed width of BU $\Delta T \pm 0.5^\circ\text{C}$ was used for calculating BU Δz because the values of the numerical derivative are very sensitive to the algorithm parameters used for evaluating the derivative. This was expected because the blow up is a discontinuous jump, and strictly speaking the derivative is undefined at that point.

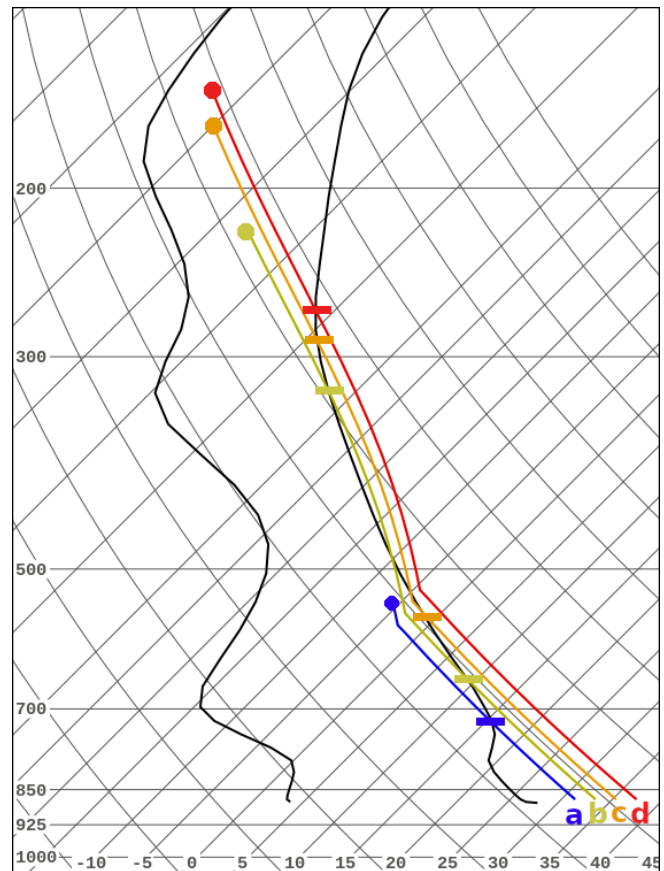


Figure 1. Four fire-heated parcels are lifted, simulating four different plumes. Horizontal lines represent where the parcels are in equilibrium with the environment (EL) and dots represent the potential maximum plume height (PMPH), where the integrated buoyancy is zero. The LCL for each parcel is obvious due to the kink in the profiles. For profiles b and c, there are two ELs due to them passing through a stable layer. In profile b, the maximum integrated buoyancy is at the lower EL, and in profile c it is at the higher EL. The black lines are the temperature and dewpoint traces from a sounding generated from model output. *Click image for an external version; this applies to all figures hereafter.*

$$IB(z) = -g \int_{SFC}^z \frac{T_p(z) - T_e(z)}{T_e(z)} dz \quad (1)$$

Equation 1. The integrated buoyancy as a function of the height (z), parcel temperature profile (T_p), and environmental temperature profile (T_e). The level where $IB(z)$ is at its maximum value corresponds to one of the equilibrium levels (if there are multiple equilibrium levels). The value of z where $IB(z) = 0$ J/kg is the maximum potential plume top.

Environment and Plume Stability

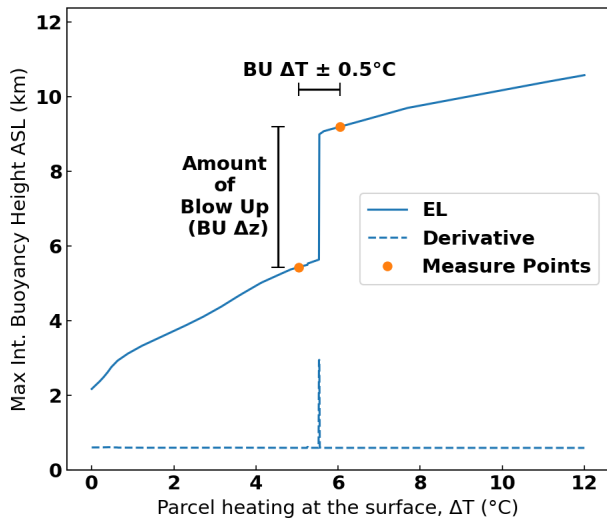


Figure 2. The equilibrium level (EL) as a function of parcel heating for the 1900 MDT 3 September 2017 model sounding at site KRR2 in Fig. 4. The Blow Up (BU) ΔT is the amount of sensible heating needed from the fire to cause the EL to jump. The amount of the blow up, or BU Δz , is defined by the difference in the EL from BU $\Delta T + 0.5^\circ\text{C}$ to BU $\Delta T - 0.5^\circ\text{C}$. In practice, the BU ΔT value is found by searching for the maximum value of the numerical derivative.

As a fire is becoming more intense, the ΔT of parcels entering the plume increases. When the jump occurs, the amount of energy in the plume does not necessarily jump quickly, but the depth of the atmosphere and the winds interacting with the fire plume do change, potentially causing a change in the fluid dynamics associated with the plume. What exactly those fluid dynamics are is beyond the scope of this paper, however, it is worthwhile to firefighters to know that the dynamics of the plume and fire behavior are changing.

There are two key parameters from Fig. 2 to watch closely when forecasting. The first is the value of the BU ΔT , or the amount of heating required to cause a blow up. The higher this value, the more heat the fire must contribute to cause a blow up. So this is a measure of the sensitivity of the plume structure to the atmospheric environment at and above the fire, and when these values are low a blow up is more likely to occur. The second parameter to watch is the BU Δz , which is a measure of how large the blow up is. Certainly a blow up of several hundred meters is not as significant as a blow up of several thousand meters. Inspection of

several of these charts during this research revealed that potential blow ups of several thousand meters are common. However, sometimes when the BU ΔT is low indicating unstable conditions, the BU Δz is also low, indicating that a potential blow up may be relatively small and insignificant for firefighter safety. So these two parameters should be used together when assessing blow up potential and severity.

Another potentially useful metric that can be gleaned from the parcel analysis is the percent of the MIB that is the result of latent heat release from the fire and the atmospheric moisture combined. The technique for partitioning the integrated buoyancy is demonstrated in Fig. 3. The dry profile is generated by continuing to lift dry adiabatically even after reaching the LCL, then the MIB from the dry profile is subtracted from the overall MIB, yielding the portion of the MIB that was due to latent heat release. Using these numbers, it is simple to calculate the percentage of the MIB that is

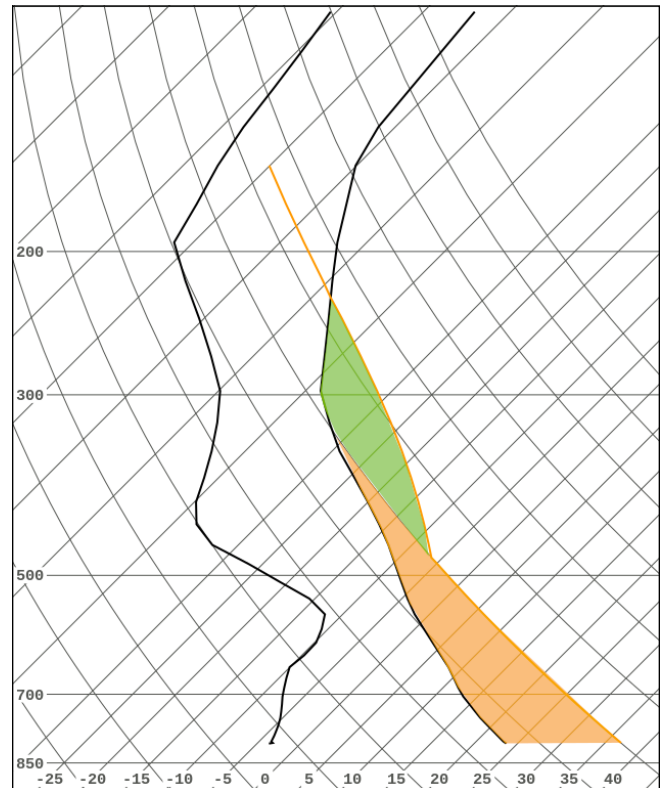


Figure 3. Shows how the integrated buoyancy is partitioned into wet and dry components. The dry component (orange) is sensible heat contributed by the fire, while the wet component (green) is contributed by latent heat release in the pyroCu cloud. The latent heat is a combination of latent heat in the atmosphere and latent heat contributed by the fire.

from latent heat release. The relevance of this metric will be discussed below.

This model is very similar to the one developed by Tory et al. (2018), but our focus is on the potential blow up of the plume EL, whereas theirs is focused on the initiation of pyroCu and pyroCb. Their model more directly accounts for the fire moisture and entrainment through specific parameters in the model. The parcel-based model proposed in this paper addresses the fire moisture by assuming a range of inputs and then looking at a range of the resulting output parameters. The model presented in this paper also simplifies the entrainment by wrapping it into the ΔT variable and using a mixed layer parcel, then ignoring entrainment as the parcel rises. As a result, this parcel-based model focuses on determining how much heating by the fire would be required to cause a blow up of the EL for plume parcels, whereas Tory et al. (2018) demonstrate the potential use of their thermodynamic model for the prediction of pyroCu and pyroCb formation. The difference between a blow up of the plume EL and the formation of a pyroCu will be discussed in more detail in section 3c below.

3. Case study demonstration

a. The Rice Ridge fire description

The Rice Ridge fire in western Montana, as seen in Fig. 4, is used as a case study to explore the proposed methods. It was discovered on 24 July 2017, and had grown to >40 000 acres by 2 September. This fire was chosen to illustrate the ideas in this paper because the surface weather conditions and fuels were similar on 2 and 3 September, but with very different fire behavior each day. The fire perimeters in Fig. 4 and the acreages reported are from the National Infrared Operations (NIROPS) program (Greenfield et al. 2003). In addition, one of the authors (Leach) was the Incident Meteorologist assigned to the fire during this period.

The surface weather and fuel conditions were similar both days, but there were different conditions in the upper atmosphere and very different fire plumes each day. This makes them good days to compare how the upper levels of the troposphere affected the fire plume. On 2 September, hot, dry, windy conditions helped the fire grow by more than 30% to almost 53 000 acres. However, some parts of the fire perimeter barely moved between 0113 MDT 2 September and 0117 MDT 3 September, which can be seen by looking

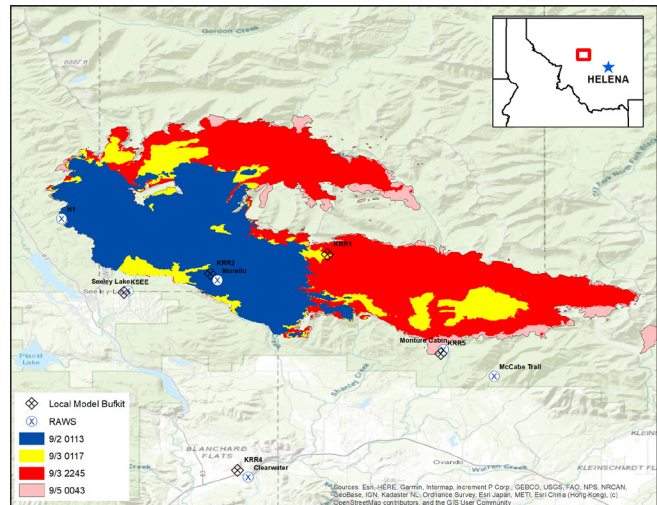


Figure 4. Map of the burn area of the Rice Ridge fire. Shading shows the fire perimeters as measured by NIROPS 2–5 September 2017. Circled X's show the location of Remote Automated Weather Stations (RAWS) (NWCG 2009), and diamonds show the locations of model soundings generated from the WRF model. Dates and times in the legend are in Mountain Daylight Time.

at the yellow area in Fig. 4. On the southern branch of the fire, there is a large portion of the perimeter that goes from blue to red in Fig. 4, which indicates the fire perimeter did not move in that area on 2 September. Then, on the evening of the 3rd, around 1900 MDT, multiple large plumes developed on the fire which almost doubled in size to more than 100 000 acres by 2245 MDT. Despite the large differences in fire growth and fire behavior each day, surface weather conditions were similar on the 2nd and 3rd. A portable weather station located at point H1 on the west end of the fire, as seen in Fig. 4, recorded maximum temperatures in the upper 80s, minimum relative humidity near 10%, and southwest winds 10–12 mph with gusts >20 mph during both afternoons. Water vapor imagery from the GOES-16 satellite accessed via the RAMMB/CIRA SLIDER (Micke 2018) shows some of the difference in the upper levels of the troposphere each afternoon as seen in Fig. 5. On the evening of 3 September (Fig. 5b), there was much more moisture aloft and multiple fire plumes across the region can be seen in the satellite image. For a more detailed analysis of the upper level atmosphere on these days, data from a retrospective weather model run were used. A detailed description of the model configuration is in appendix A. Model simulations were initialized at 0000 UTC each day 28

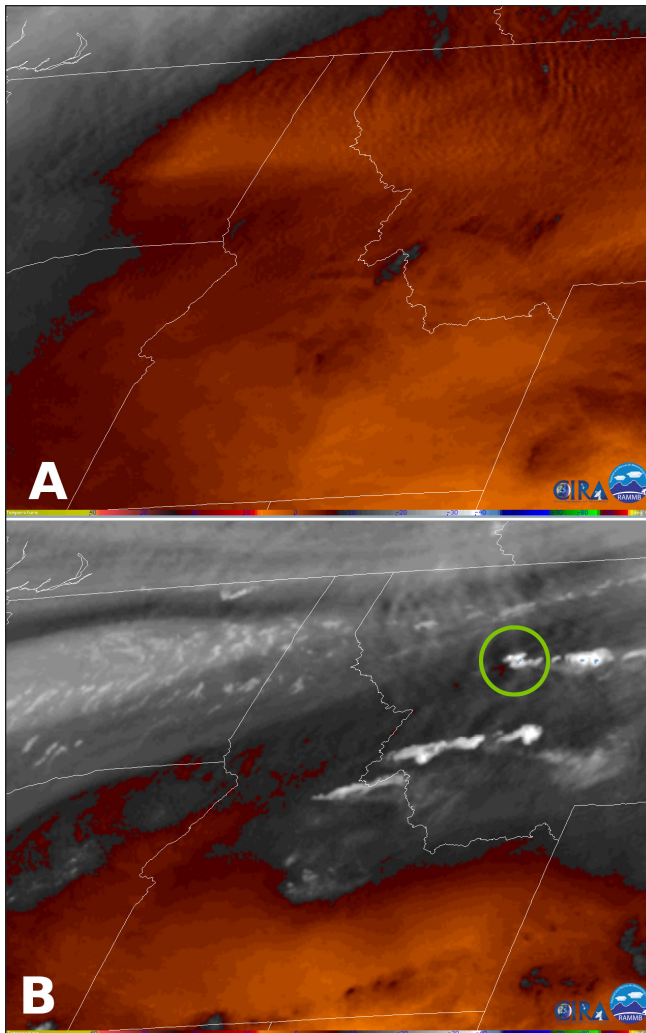


Figure 5. Midlevel water vapor imagery from channel 9 ($6.9 \mu\text{m}$) of GOES-16 satellite at 0300 UTC 3 September 2017 (A) and 0400 UTC 4 September 2017 (B). The green circle in panel B shows the location of the pyroCu associated with the Rice Ridge fire. Other fire plumes can be seen on the same day in panel B located in central Idaho and southwestern Montana.

August through 4 September and simulated 24 hours of weather. When necessary to create a longer time series of data, the different model runs were stitched together end-to-end to provide a longer time series.

b. Analysis and discussion of the Rice Ridge fire

Most existing methods of assessing stability are ineffective for wildfires because they neglect the role of the heat and moisture contributed by the fire, and in some cases they neglect moisture altogether. For instance, just using low-level environmental lapse rates ignores

the fire plume as well as moisture produced by the fire and in the environment. Using CAPE alone or any other index tuned for thunderstorms also ignores the role of the wildfire. Indices that are sensitive to low-level atmospheric moisture do not recognize dry environments conducive to wildfire occurrence and rapid growth. Further, they do not allow for the interpretation of the pyroCu cloud if and when it forms. Is the pyroCu a precursor to a blow up or just a cloud at the top of the fire plume? While Tory et al. (2018) does focus on pyroCb initiation and heat released by the fire, their model does not always provide context for interpreting pyroCu clouds. On the Rice Ridge fire, the low-level lapse rates from 800 hPa to 700 hPa from the WRF model at site KRR2 (Fig. 4) were $9.7^\circ\text{C}/\text{km}$ and $9.4^\circ\text{C}/\text{km}$ at 1900 MDT on 2 September and 3 September, respectively. At the same time, neither sounding showed any CAPE. Others have also reported on the limitations of using CAPE for wildfire analysis (Potter et al. 2006; Trentmann et al. 2006; Fromm et al. 2010; Potter and Anaya 2015).

Figure 6 applies the proposed model to the Rice Ridge case by comparing the conditions on 2 September and 3 September. It is similar to Fig. 2, except shading is used to indicate a range of values due to uncertainty related to the amount of moisture released by the fire, which will be discussed in more detail in section C below. Figure 6 also shows the LCL, and when the plume reaches the LCL there is a pyroCu present. Using Fig. 6, it is evident that the evening of 3 September (Fig. 6b) was much more unstable than the evening of 2 September (Fig. 6a) because the blow up, or jump in the EL, occurs at a lower value of parcel heating, or ΔT .

Figure 6c compares the model soundings on the evenings of 2 and 3 September. The model soundings show similar conditions from about 700 hPa down to the surface, which agrees well with surface observations that the surface weather was similar those two days. However, on 3 September, the model shows much more moisture above 700 hPa, which matches well with the water vapor imagery in Fig. 5. Close inspection of the model soundings in Fig. 6c suggests 500 hPa level temperatures cooled by 2.8°C from the evening of 2 September to the evening of 3 September, and comparison with North American Regional Reanalysis data (Mesinger et al. 2006) agrees well with about 2°C of cooling. These comparisons don't fully validate the model simulation's accuracy; however, they show at least a qualitative agreement between the observations and the simulations.

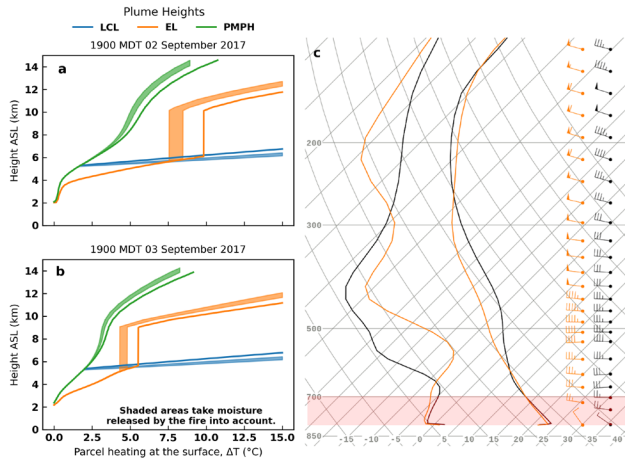


Figure 6. Plots of the LCL, EL, and potential maximum plume height (PMPH) versus heating for (a) 1900 MDT 2 September 2017 and (b) 1900 MDT 3 September 2017 on the Rice Ridge fire. These were calculated using model soundings from site KRR2 in Fig. 4. The single lines assume no moisture, or latent heat, is contributed by the fire while the shaded areas account for a range of moisture released by the fire. The model sounding in black on panel c is for 2 September and corresponds to panel a, and the model sounding in orange on panel c is for 3 September and corresponds to panel b. The red shading indicates the 100hPa layer used for calculating the initial mixed layer parcel.

So, though both days had similar weather conditions at the surface, the conditions aloft were significantly different, allowing a stronger plume to develop on the 3rd. Figure 7 shows a time series of the blow up ΔT and Δz values along with highlighting of the two periods being compared. A blow up occurred on 3 September as the BU ΔT was rapidly dropping and approaching a minimum while the BU Δz remained high, indicating a potential blow up of several kilometers. In Fig. 7, the orange line labeled pyroCu shows the amount of heating required to reach the LCL, and thus the amount of heating required for a pyroCu to first form.

c. The dependent pyroCu as a visual indicator

Plotting the LCL and PMPH as in Fig. 6 gives useful information about the meaning of a pyroCu cloud should one be observed atop a plume. Once the LCL is below the PMPH, there is a pyroCu cloud on the top of the plume, as in profile a from Fig. 1. Figure 6a shows that for 2 September, once a pyroCu cloud is observed, there is still a considerable amount more heating necessary to

cause a blow up. So, on 2 September the appearance of a pyroCu cloud atop the plume is by itself not a cause for concern about a blow up. However, on 3 September as seen in Fig. 6b, if a pyroCu cloud is observed, it is an indicator that the fire output is closer to hot enough to produce a blow up, and it is cause for caution. The same information can be more easily gleaned by looking at the spacing between the lines labeled “Blow Up ΔT ”

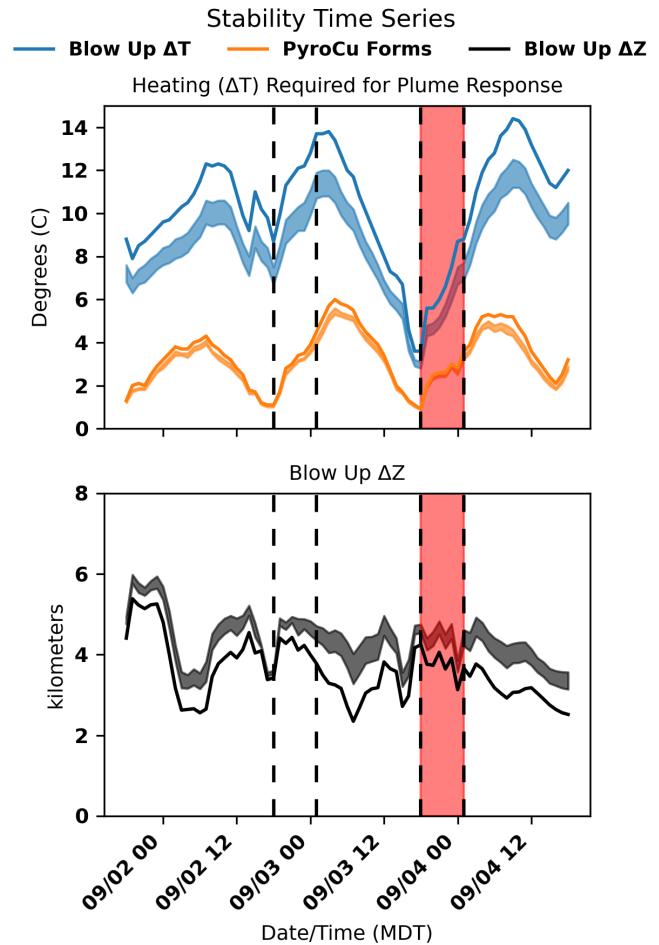


Figure 7. A time series of the BU ΔT , the ΔT at which a pyroCu first appears, and BU Δz at point KRR2 in Fig. 4 during the Rice Ridge Fire. The first time period highlighted by the dashed vertical lines is the evening of 2 September through about 0100 MDT when no blow up occurred. The second period with the red shading is the evening of 3 September when a blow up did occur with similar surface conditions as were present on 2 September. The pyroCu line in the top panel shows the amount of heating required to initiate a pyroCu cloud. The distance between the blue and orange lines indicates the difference in heating needed to initiate a pyroCu versus causing a blow up.

and “PyroCu Forms” on Fig. 7. The closer together those lines are, the less additional heating is required to go from pyroCu to blow up. When the LCL is below the PMPH but above the EL as in sounding a in Fig. 1, then a pyroCu cloud only exists as part of the overshooting top of the plume and is totally dependent on the fire plume driving it from below. Once the LCL drops below the EL, then latent heat release in the cloud contributes to the MIB and also affects the EL. Profile d in Fig. 1 is a good example of a profile where the LCL is below the EL. For profiles b and c in Fig. 1, whether pyroCu is considered dependent or not depends on which level is chosen as the EL, as discussed in section 2. The LCL typically, but not always, drops below the EL at similar ΔT values as the blow up of the EL, as seen in Fig. 6a and 6b.

d. *Balancing sensible and latent heating*

When there is no pyroCu cloud, the plume is driven from the surface by sensible heating. However, once a cloud forms and there is latent heat release, then the plume is at least partially driven in a manner similar to a convective cloud or thunderstorm. The fluid dynamics of these situations are beyond the scope of this paper; however, understanding whether sensible heating or latent heating dominates, or whether they are well balanced, could be valuable information for firefighters. A transition between a plume-driven by surfaced-based sensible heating to one dominated by latent-heat release aloft, or even one that is balanced between the two, likely represents a significant change in the plume dynamics. The elevated latent heat release mechanism is well studied by meteorologists in the context of convective clouds and thunderstorms. Plumes driven by sensible heating from the surface have also been studied e.g., Briggs (1965). However, the dynamics of scenarios where both are present are not well understood and thus represent a potentially dangerous situation.

The percentage of heat in the plume that is released via latent heat can be considered on a spectrum from 0% to 100%. On the low end, near 0%, the fire is driven by sensible heating at the surface and the plume should be reasonably well-modeled by the Briggs (1965) plume model. At the other end of the spectrum, the plume is dominated by latent heat release aloft and should be expected to behave similarly to a convective cloud or thunderstorm, similar to cases studied by Cunningham and Reeder (2009). The fluid dynamics in the middle of the spectrum are largely unknown. For instance, it

is well known that thunderstorms cause changes in the atmospheric pressure and wind fields near the surface, leading to erratic winds, which is why firefighters are taught about thunderstorm winds as “critical winds” in the Intermediate Wildland Fire Behavior Course, S-290 (S-290 2010). If similar changes in a plume with significant latent heat release aloft enhanced the surface fire, it could set up a positive feedback where the surface fire grows stronger and supports the pyroCu cloud.

Figure 8 shows the balance between the wet and dry components of the MIB as a function of fire heating for 2 September and 3 September. On the 3rd, the contributions from latent heat release rose to 20–40% of the energy released in the plume, indicating that latent heat release in the upper levels was a significant contribution to the overall energy in the plume. It is also noteworthy that in the case of this metric, accounting for the moisture released from the fire also has a significant impact.

e. *Impact of including moisture in the analysis*

For the proposed model, including moisture released by the fire was found to have significant effects on the results. In Table 1, the MIB is calculated at the BU $\Delta T + 0.5^\circ\text{C}$ to get the MIB after the blow up, and this means that the MIB in each case is different. Including moisture causes significant proportional decreases in the amount of fire heating required to trigger a blow up as shown in

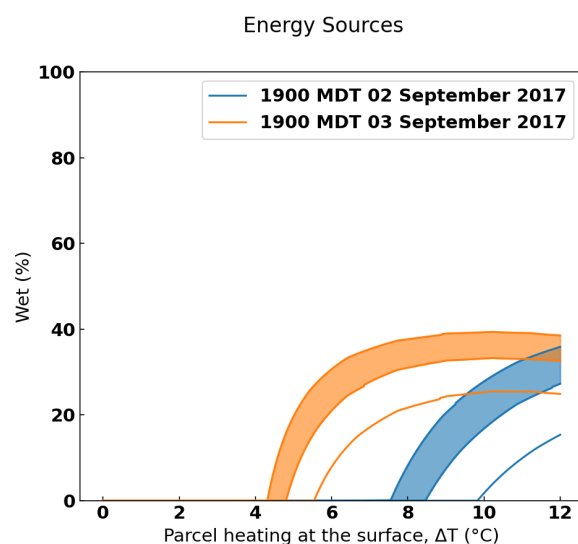


Figure 8. The balance between the wet and dry components of the MIB. Shaded areas take moisture from the fire into consideration.

Table 1. The impact of including fire-released moisture when evaluating the parcel-based model for the Rice Ridge Fire. The last row shows the percent of the MIB that is from latent heat release.

Date:	2 September 2017			3 September 2017		
Moisture Added	0 g/kg	1 g/kg per 15°C heating	1 g/kg per 8°C heating	0 g/kg	1 g/kg per 15°C heating	1 g/kg per 8°C heating
BU ΔT (C)	9.9	8.5 (–14%)	7.6 (–23%)	5.6	4.8 (–14%)	4.3 (–23%)
MIB at BU $\Delta T + 0.5^\circ\text{C}$ (J/kg)	1064	901 (–15%)	808 (–24%)	510	424 (–17%)	381 (–25%)
Percent MIB from Latent Heat at BU $\Delta T + 0.5^\circ\text{C}$ (%)	5	7	10	9	12	16

Table 1. It also caused a significant decrease in the MIB buoyancy after the blow up, despite the EL and PMPH being higher as depicted in Fig. 6. This unintuitive result is because of taller, thinner profiles in a skew-T log-P diagram right after the blow up when moisture from the fire is considered. These blow ups occur with less sensible heating, and the extra heat contributed as latent heat is not enough to cause a more energetic blow up.

For the Rice Ridge fire, including moisture had a large impact on some of the analyzed parameters. Figure 6 shows the heights of LCLs, ELs, and PMPHs for the point KRR2 at Rice Ridge on the evenings of 2 September and 3 September. The solid lines show the results of the parcel-based model without accounting for moisture released by the fire, and the shaded areas account for a range of moisture. It is noticeable that the impact of the moisture on the relative heights is small in most cases, especially the LCL, which agrees well with Luderer et al. (2009). However, the moisture does have a significant effect on the amount of heating required to trigger a blow up, especially on the more stable day, 2 September. On 3 September, the more unstable day, the moisture also lessens the amount of heating required but by a smaller margin. That is the typical pattern for these plots; on the most unstable days fire moisture is a relatively minor contributing factor to the instability. However, Fig. 8 shows that accounting for the moisture can have a big impact on the balance of where and how the energy in the plume is released. From Table 1 it is apparent that even on 3 September accounting for moisture released from the fire shifted the balance from 9% of the energy coming from latent heat release up to 12–16%.

4. Limitations and applications of the parcel-based model

a. Limitations of the parcel-based model

One of the weaknesses of most parcel-based models is that they do not account for wind. Early on in the research of blow up fires, Byram (1954) proposed the importance of the wind profile, and specifically the balance between the winds and the fire power. Potter (2012a) summarizes the current state of understanding in this area well and adds emphasis to Byram's observations about the wind direction profile. Lareau and Clements (2016) briefly discusses the wind profile and shear as well in an observed case where the shear overcomes the instability and tears the plume apart. Vertical wind shear will also cause the plume to tilt in the down-shear direction (Briggs 1965), which could affect the plume dynamics and any potential feedback mechanisms such as long-range spotting.

Another weakness of the parcel-based model used here is that it ignores entrainment. Peterson et al. (2017) showed that for several cases of intense surface fire, the strongest selector of the environmental variables he investigated for differentiating between a fire with a pyroCb and one without was the midlevel moisture in the atmosphere. Comparing the upper level moisture between 2 and 3 September as in Fig. 5 and Fig. 6c, dry air entrainment aloft may have also been a significant factor for the case discussed here which is not handled by our parcel-based model. Modeling efforts by Trentmann et al. (2006) also showed most of the air in the upper levels of the plume was entrained from the environment. Tory et al. (2018) investigated the rates of entrainment within the parcel-based model they developed. They showed that for a plume with a core

that had zero entrainment, the condensation level for a pyroCb would be deep in the stratosphere. Large eddy simulations they conducted showed that the pyroCb clouds condensed near the environmental condensation level, which implies that the plumes were diluted by 95% or more in a hot, dry atmosphere. Their simulations indicated that most of the entrainment occurred in the lower portion of the plume, and that cross sections of the plumes showed cores of less diluted air. So even though the plumes are much diluted, the cores of the plumes are relatively less diluted. As a result, for a plume to develop a pyroCb, the surface fire must be powerful and spatially extensive enough to initially develop a sufficiently large core of buoyant plume gases.

As a result, predicting whether a pyroCb will form would require detailed information about the surface fire and rates of entrainment expected, which is not currently possible. Indeed, a sensitivity analysis by Luderer et al. (2006) using a plume model showed that sensible heat, or fire power, was the most important factor for determining whether intense pyroconvection formed in the case they studied. However, by analyzing the thermodynamics of parcels with various amounts of sensible heat added (and thus various values for ΔT), the degree of supportiveness of the atmosphere for intense pyroconvection can be evaluated. This information can be useful for forecasting trends and highlighting periods of increased risk to wildland firefighters and the public, but once the stability is assessed and high risk is the result, other factors such as wind shear, entrainment, and fuels will also need to be taken into consideration. Surface weather conditions and their effect on fire intensity are also not considered. The parameters presented here only describe the thermodynamic considerations of how the atmosphere will suppress or enhance a fire plume, but ultimately the fire must produce enough heat to create a blow up. Fire behavior will change with surface weather conditions such as wind, solar insolation, temperature, and humidity as well as terrain influences and the amount of available fuel. As a result of this limitation, time series of BU ΔT and BU Δz should be used to assess trends in stability. A meteorologist should work closely with a fire behavior specialist to assess the impacts of fuels, surface weather, and terrain to determine any trends in fire intensity and produce the final assessment of the risk of a blow up.

A lack of available fire data means that the model also cannot be evaluated in a statistical manner that would support quantitative use of BU ΔT and BU Δz . Availability of weather datasets such as the North

American Regional Reanalysis data (Mesinger et al. 2006) provide ample weather data for a more robust analysis, but the data on fire plumes are lacking. Although large plumes on fires are frequently reported in the media when they occur, the null cases when there is a powerful fire that does not produce a large plume are not generally documented. For the case of the Rice Ridge fire, one of the authors (Leach) was the incident meteorologist on the fire with firsthand observations. Furthermore, while inspecting many atmospheric soundings during this research it became evident that although nearby locations showed similar trends, the quantitative values were often significantly different.

b. Applications of the parcel-based model

Using this model gives the appearance of a pyroCu on a plume utility for forecasting short term fire behavior. It allows the onsite meteorologist or fire behavior specialist to estimate how strong the fire is, and using this information and a diagram like those in Fig. 6 and Fig. 7, assess how near the fire plume is to a blow up. If this approach was used ahead of time for the Rice Ridge Fire, this knowledge could have been useful to communicate that if on 2 September the pyroCu had appeared, it would have indicated that the fire was only producing about $\frac{1}{4}$ to $\frac{1}{3}$ of the necessary power to cause a blow up. However, on 3 September it would indicate that the fire was closer to producing a blow up. This can be seen most clearly by looking at the separation between the blue “Blow Up ΔT ” and orange “PyroCu Forms” lines in Fig. 7. So this model is useful for providing context and giving a more practical interpretation of the appearance of a pyroCu on the top of a fire plume.

The limitations discussed in section 4a above preclude direct, quantitative application of the BU ΔT and BU Δz for predicting a blow up, however, they can be used to assess trends in the atmospheric factors affecting the stability of wildfire plumes. Figure 9 is the same as Fig. 7 but for a longer time period. The afternoons of 29 and 30 August are highlighted in addition to the time periods on 2 and 3 September that have already been discussed. The BU ΔT on both days is zero or very near zero, which happens when the surface temperature is warm enough to cause convection without the addition of heat added by a wildfire. Both of these days also had large fire plumes on the southwestern edge of the fire near Seeley Lake and the station KSEE in Fig. 4. The incident management team responded both days with

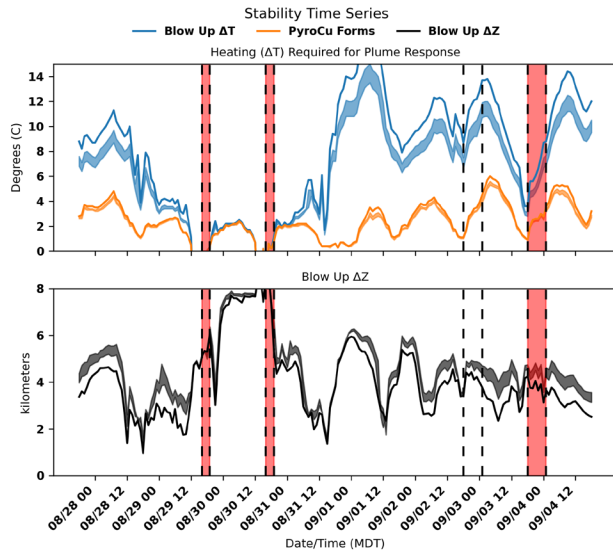


Figure 9. The same as Fig. 7 but for a longer time series starting the evening of 27 August. The first two periods of interest shown by the pairs of vertical dashed lines with red shading also had large fire plumes. The latter two periods are the same as in Fig. 7 for reference.

large air tankers to suppress the fire near threatened structures. These days were not suited for the discussion in section 3 because the fire plumes were in a different location on the fire and the surface weather conditions were very different when compared to the days that there were no large fire plumes. As a result, the role of the stability cannot be evaluated in relative isolation as it can be when comparing 2 and 3 September. However, looking at the time series in Fig. 9, it is clear that the atmosphere would become less supportive of large plumes on 31 August, and much less supportive of large plumes for the first few days of September. This information, along with forecast surface weather conditions and the fuels conditions, can be combined to provide a qualitative assessment of the risk of a blow up and large fire plume.

Whereas the specific values of BU ΔT and BU ΔZ varied from location to location, the general trends were similar at many locations across the region on 2 and 3 September. And there were several larger fire plumes observed across the region on the 3rd compared to the 2nd. Some of these can be seen in Fig. 5b, and several could also be seen on the KMSX Doppler radar.

5. Summary and conclusions

A simple parcel-based model for assessing the atmospheric aspects affecting the potential for large

wildfire plumes was developed and applied to the Rice Ridge fire near Seeley, Montana in 2017. In the model, if a fire produces enough heat, the equilibrium level of parcels in the plume suddenly jumps to a much higher level. This sudden change, called a blow up, represents a sudden change in the fire plume and potentially the fluid dynamics of the plume and fire environment, though those aspects are not discussed in this paper.

The model predicts that on two days with similar surface weather and fuel conditions, differences in the atmosphere far above the surface can have a large impact on the size of the fire plume that develops. Applying the model to 2 and 3 September 2017 on the Rice Ridge fire and comparing the results to the observed fire behavior supports these predictions.

The role of moisture released by the wildfire is also assessed. Within the proposed parcel-based model, heat energy is released at the surface via sensible heat transfer from the fire, and latent heat is released in the fire plume via condensation in a pyroCu cloud. It was found that whether or not the latent heat contributed by combustion was accounted for in the model could have a large impact on the analyzed balance between how much energy was released at the surface and how much was released in the pyroCu aloft. It is the authors' opinion that the balance between the energy released at the surface and the energy released in the cloud may have a large impact on the dynamics of the fire plume, though these ideas are beyond the scope of this paper and not further developed.

Furthermore, the relationship between the presence of a pyroCu cloud and a blow up of the equilibrium level is briefly discussed. The model shows that in some cases, a pyroCu is an immediate predecessor to a blow up because relatively little additional heat is needed in the plume to trigger a blow up. In other cases, the difference in heating required to create a pyroCu and a blow up is large enough that the presence of a pyroCu is not cause for concern about a blow up.

The parcel-based model proposed in this paper can be used to assess trends in atmospheric stability as it relates to wildfire plumes. Because of the lack of available data on fire plumes, an in-depth analysis of the proposed parcel-based model would be very difficult, and thus quantitative applications are not recommended until a broader evaluation using more fires is completed. However, by observing trends in the BU ΔT and BU ΔZ and fire behavior, forecasters can assess trends in the atmosphere specifically as they relate to fire plumes. Furthermore, the model provides a means to interpret

the appearance of a pyroCu cloud on the top of a fire plume. Application of this model could potentially give forecasters a tool to make forecasts such as:

- “If you see a pyroCu develop today, the fire plume is unlikely to blow up soon and show a dramatic change in behavior. It will take a lot more intense fire to produce a blow up than to create a pyroCu today.”
- “If the fire burns in similar fuels and terrain tomorrow, it is much more/less likely to blow up than it was today.”
- “The atmosphere is relatively stable and likely won’t support deep plume development or a blow up fire for the next three days, but then conditions become much, much more unstable.”

Finally, this tool is not intended to be a stand-alone index per se, but rather a means to evaluate trends in atmospheric stability and the potential for the atmosphere to hinder or support the development of large fire plumes. Many other variables need to be

considered by fire behavior experts, such as changing surface weather conditions, changing fuel conditions, suppression activities, and movement of the fire into different terrain and fuel regimes. This tool has potential to assist in the conversation between fire meteorologists, fire behavior experts, and decision makers.

Acknowledgments. First, we would like to thank Jason Forthofer and Natalie Wagenbrenner of the Missoula Fire Science Lab for discussions on wildfire plumes and the opportunity to present our research via their seminar series. In addition, we would like to thank Meteorologist in Charge, Bruce Bauck of the National Weather Service in Missoula Montana for his support on this project. Thanks are also due to Kevin Tory of the Science and Innovation Group, Bureau of Meteorology, and Bushfire and Natural Hazards Cooperative Research Centre for email discussions helping us to better understand the significance of the fire released moisture to the plume thermodynamics. Finally, reviewers of the initial paper were very helpful, and the article is much improved by incorporation of their feedback.

APPENDIX A

SWRF-Model Configuration

Modeling for this study utilized the Unified Environmental Modeling System, or UEMS-WRF version 20.8.2, utilizing the NCAR-ARW core. Many references for mesoscale Numerical Weather Prediction systems are available, including Gallus and Bresch (2006). Data from the Global Forecast System (GFS) (Environmental Modeling Center 2003; Kalnay et al. 1990) were utilized for lateral and boundary condition initialization. In this case, archived GFS analysis data utilizing the GDAS data assimilation system are available every three hours at a grid point resolution of 0.5° degrees of latitude (approximately 54 km).

UEMS-WRF runs were initialized at 0000 UTC on 28, 29, 30 and 31 August 2017 and 1, 2, 3 and 4 September 2017. Each run was completed for 24 hours, matching the GFS analysis as boundary conditions, and utilizing an adaptive time step. Three nests were configured, centered on Seeley, Montana at 47.176°N , 113.444°W .

Parent Domain:

$\text{NX} \times \text{NY} = 110 \times 110$

Grid Spacing = 18 km

Nested Domain 1

$\text{NX} \times \text{NY} = 100 \times 100$

Grid Spacing = 6 km

Nested Domain 2

$\text{NX} \times \text{NY} = 100 \times 100$

Grid Spacing = 2 km

Data were post-processed into BUFKIT style sounding (profiles) for points of interest, collocated with surface weather observing stations.

Further model configuration included a Multi-Scale Kain-Fritsch cumulus parameterization scheme (Kain 2004) for the parent domain and no cumulus parameterization schemes running for the nests. The planetary boundary layer scheme used for all domains is Yonsei University (Skamarock et al. 2008). Microphysics for all domains utilized the Lin et al. scheme, most recently referenced by Chen and Sun (2002). The Unified NOAA Land Surface Model are used (Chen and Dudhia 2001) and the Rapid Radiative Transfer Model (RRTM) Radiation Scheme (Mlawer et al. 1997).

REFERENCES

- American Meteorological Society, 2021: Pyrocumulonimbus. Glossary of Meteorology, [CrossRef](#).
- Briggs, G. A., 1965: A plume rise model compared with observations. *Journal of the Air Pollution Control Assoc.*, **15**:9, 433–438, [CrossRef](#).
- Byram, G. M., 1954: Atmospheric conditions related to blowup fires. USDA Forest Service, Southeastern Forest Experiment Station, Paper 35. (Asheville, NC), [CrossRef](#).
- Chen, F., and J. Dudhia, 2001: Coupling an advanced land surface-hydrology model with the Penn State-NCAR MM5 modeling system. Part 1: Model implementation and sensitivity. *Mon. Wea. Rev.*, **129**, 569–585, [CrossRef](#).
- Chen, S. H., and W. Y. Sun, 2002: A one-dimensional time dependent cloud model. *J. Meteor. Soc. Japan*, **80**, 99–118, [CrossRef](#).
- Cunningham, P., and M. J. Reeder, 2009: Severe convective storms initiated by intense wildfires: Numerical simulations of pyro-convection and pyro-tornadogenesis. *Geophys. Res. Lett.*, **36**, L12812, [CrossRef](#).
- Doswell, C. A. III, 2001: *Severe Convective Storms – An Overview*. *Severe Convective Storms*, Meteorological Monographs, **28**:50, American Meteorological Society, 1–26.
- Ebert, C. H. V., 1963: The meteorological factor in the Hamburg fire storm. *Weatherwise*, **16**, 70–75, [CrossRef](#).
- Environmental Modeling Center, 2003: The GFS Atmospheric Model. NCEP Office Note 442, Global Climate and Weather Modeling Branch, EMC, Camp Springs, Maryland.
- Fromm, M., D. T. Lindsey, R. Servranckx, G. Yue, T. Trickl, R. Sica, P. Doucet, and S. Godin-Beekmann, 2010: The untold story of pyrocumulonimbus. *Bull. Amer. Meteor. Soc.*, **91**, 1193–1210, [CrossRef](#).
- Gallus, W. A. Jr. and J. F. Bresch, 2006: Comparison of impacts of WRF Dynamic Core, physics package, and initial conditions on warm season rainfall forecasts. *Mon. Wea. Rev.*, **134**, 2632–2641, [CrossRef](#).
- Goens, D. W. and P. L. Andrews, 1998: Weather and Fire Behavior Factors Related to the 1990 Dude Fire Near Payson, Arizona. *Preprints, 2nd Conference on Fire and Forest Meteorology*, Phoenix, AZ, Amer. Met. Soc., 6.6, [CrossRef](#).
- Greenfield, P. H., W. Smith, and D. C. Chamberlain, 2003: Phoenix — the new Forest Service airborne infrared fire detection and mapping system [online]. In *2nd International Wildland Fire Ecology and Management Congress and 5th Symposium on Fire and Forest Meteorology*, Orlando, FL. Amer. Met. Soc. p. J1G.3. Available from https://ams.confex.com/ams/FIRE2003/techprogram/paper_66675.htm [accessed 25 February 2021].
- Kain, J. S., 2004: The Kain-Fritsch Convective Parameterization: An update. *Journal of Applied Met.*, **43**, 170–181, [CrossRef](#).
- Kalnay, E., M. Kanamitsu, and W. E. Baker, 1990: Global numerical weather prediction at the National Meteorological Center. *Bull. Amer. Meteor. Soc.*, **71**, 1410–1428, [CrossRef](#).
- Lareau, N. P., and C. B. Clements, 2016: Environmental Controls on Pyrocumulonimbus Initiation and Development. *Atmos. Chem. Phys.*, **16**, 4005–4022, [CrossRef](#).
- _____, N. J. Nauslar, and J. T. Abatzoglou, 2018: The Carr Fire vortex: A case of pyrotornadogenesis? *Geophysical Research Letters*, **45**, 13107–13115, [CrossRef](#).
- Lin, Y.-L., R.D. Farley, and H.D. Orville, 1983: Bulk parameterization of the snow field in a cloud model. *J. Climate Appl. Meteor.*, **22**, 1065–1092, [CrossRef](#).
- Luderer, G., J. Trentmann, and O. M. Andreae, 2009: A new look at the role of fire-released moisture on the dynamics of atmospheric pyro-convection. *International Journal of Wildland Fire.*, **18**, 554–562, [CrossRef](#).
- _____, _____, T. Winterrath, C. Textor, M. Herzog, H. F. Graf, and M. O. Andreae, 2006: Modeling of biomass smoke injection into the lower stratosphere by a large forest fire (Part II): sensitivity studies. *Atmos. Chem Phys.*, **6**, 5261–5277, [CrossRef](#).
- Mesinger, F., and Coauthors, 2006: North American regional reanalysis. *Bull. Amer. Meteor. Soc.*, **87**, 343–360, [CrossRef](#).
- Micke, K., 2018: Every pixel of GOES-17 imagery at your fingertips. *Bull. Amer. Meteor. Soc.*, **99**, 2217–2219, [CrossRef](#).
- Mlawer, E. J., S. J. Taubman, P. D. Brown, M. J. Iacono and S.A. Clough, 1997: Radiative transfer for inhomogeneous atmospheres: RRTM, a validate correlated-k model for the longwave. *J. Geophysical Res.*, **102**, 16663–16682, [CrossRef](#).
- NWCG, 2009: Interagency Wildland Fire Weather Station Standards and Guidelines. NWCG PMS 426-3, August 2009, 64 pp.
- Peterson, D. A., E. J. Hyer, J. R. Campbell, M. D. Fromm, J. W. Hair, C. F. Butler, and M. A. Fenn, 2015: The 2013 Rim Fire: Implications for predicting extreme fire spread, pyroconvection, and smoke emissions. *Bull. Amer. Meteor. Soc.*, **96**, 229–247, [CrossRef](#).
- _____, _____, _____, J. E. Solbrig, and M. D. Fromm, 2017: A conceptual model for development of intense pyrocumulonimbus in Western North America. *Mon. Wea. Rev.*, **145**, 2235–2255, [CrossRef](#).
- Potter, B. E., 2002: A dynamics based view of atmosphere-fire interactions. *International Journal of Wildland Fire*, **11**, 247–255, [CrossRef](#).
- _____, 2005: The role of released moisture in the atmospheric dynamics associated with wildland fires. *International Journal of Wildland Fire*, **14**, 77–84, [CrossRef](#).

- _____, 2012a: Atmospheric interactions with wildland fire behaviour – I. Basic surface interactions, vertical profiles and synoptic structures. *International Journal of Wildland Fire*, **21**(7), 779–801, [CrossRef](#).
- _____, 2012b: Atmospheric interactions with wildland fire behavior – II. Plume and vortex dynamics. *International Journal of Wildland Fire*, **21**, 802–817, [CrossRef](#).
- _____ and M. A. Anaya, 2015: A wildfire-relevant climatology of the convective environment of the United States. *International Journal of Wildland Fire*, **24**, 267–275, [CrossRef](#).
- _____, J. J. Charney, and L. A. Fusina, 2006: Atmospheric moisture's influence on fire behavior: surface moisture and plume dynamics. *International Conference on Forest Fire Research*, [CrossRef](#).
- S-290 Intermediate Wildland Fire Behavior Course. The source of this material is the COMET® Website at meted.ucar.edu/ of the University Corporation for Atmospheric Research (UCAR), sponsored in part through cooperative agreement(s) with the National Oceanic and Atmospheric Administration (NOAA), U.S. Department of Commerce (DOC). ©1997–2017 University Corporation for Atmospheric Research. All Rights Reserved.
- Skamarock, W. C., J. B. Kemp, J. Dudhia, D. O. Gill, D. Barker, W. Wang, and J. G. Powers, 2008: A Description of the Advanced Research WRF Version 3 (No. NCAR/TN-475+STR). University Corporation for Atmospheric Research, [CrossRef](#).
- Tory, K. J., W. Thurston, and J. D. Kepert, 2018: Thermodynamics of pyrocumulus: A conceptual study. *Mon. Wea. Rev.*, **146**, 2579–2598, [CrossRef](#).
- Trentmann, J., and Co-authors, 2006: Modeling of biomass smoke injection into the lower stratosphere by a large forest fire (Part I): Reference simulation. *Atmos. Chem. Phys.*, **6**, 5247–5260, [CrossRef](#).
- WMO, 2017: *International Cloud Atlas*. Accessed 3 July, 2020, [CrossRef](#).